International Journal of Multiphase Flow 34 (2008) 809–818

Contents lists available at ScienceDirect

International Journal of Multiphase Flow

journal homepage: www.elsevier.com/locate/ijmulflow

Equivalent water layer height (EWLH) measurement by a single-wire capacitance probe in gas–liquid flows

Shanfang Huang *, Xiugang Zhang, Dong Wang, Zonghu Lin

State Key Laboratory of Multiphase Flow in Power Engineering, Xi'an Jiaotong University, Xi'an 710049, PR China

ARTICLE INFO

Article history:
Received 15 November 2007
Received in revised form 24 February 2008
Available online 29 March 2008

Keywords:
Equivalent water layer height (EWLH)
Gas–liquid flows
Single-wire capacitance probe
Bubble size
Interfacial velocity

ABSTRACT

The objective of this study was to measure EWLH in horizontal pipes by a single-wire capacitance probe. The capacitance measured by the probe is linearly proportional to EWLH with a high sensitivity of 1.52 pF/mm. The measurements are independent of water salinity, phase distribution, and wire shape. The static performance of the probe was validated theoretically and experimentally. In dynamic process, the parameters relevant to fluids and wire influence the measuring accuracy of EWLH, but the errors are constant and small. For the given wire and fluids, the accuracy decreases as bubble size decreases or interfacial velocity increases, which is mainly relevant to flow patterns.

Time traces of EWLH in all the flow patterns were obtained, from which the flow parameters were estimated such as interfacial velocities, phase distributions, void fractions, and flow patterns. The measuring accuracy is high in stratified and intermittent flows, but low in bubbly and annular flows. However, the time traces can reflect the flow characteristics in all the flow patterns, and the statistical parameters of the time traces were different from each other.

1. Introduction

In horizontal gas–liquid two-phase flows, water layer height is an important parameter to reflect flow structure and the concerned parameters such as interfacial velocities, phase distributions, void fractions, and flow patterns. Thus there are many methods to measure EWLH such as visual observation, X-ray or γ-ray radiation, hot wire anemometry, electrical probes, and etc. Among the methods, electrical probes, depending on the different conductivity or capacitance between phases, are the most popular for the sake of convenience, economics and safety.

Electrical technique includes non-intrusive and intrusive probes. The electrodes are mounted peripherally around the flow field for the non-intrusive probes. On the contrary, the electrodes of the intrusive ones are placed into the flow field to contact with the fluids directly. Compared with the signals of the former, the signals of the latter are more dependent on the flow field and independent of the environments. Conte and Azzopardi (2003) reviewed different kinds of intrusive probes, e.g. needle-contact probe, parallel-wire probe and flush-wire probe. Among the three, parallel-wire probe is the most widely used in gas–liquid two-phase and gas–liquid–liquid three-phase flows (Lunin-ski et al., 1983; Andritsos and Hanratty, 1987; Shi and Kocamustafaogullari, 1994; Oddie et al., 2003). However, flush-wire probe is proved to be the best from the aspect of spatial resolution by experiments and numerical simulations (Kang and Kim, 1992a,b).

By the electrical techniques mentioned above, much progress has been made on measurement of water layer height in multiphase flows. However, the methods are subject to the variation of water conductance and water distribution since the conductivity between electrodes is measured directly. Therefore, a single-wire capacitance probe was used by Fagundes Netto et al. (1999) and Huang et al. (2007). The capacitance probe is able to measure water layer height effectively and is independent of water salinity or its distribution. Fagundes Netto et al. (1999) measured water layer height in elongated-bubble flows and the time traces were consistent with the flow structures completely. Time-averaged water holdup based on the EWLH in kerosene–water two-phase flows was obtained over the cross section of the pipe (Huang et al., 2007).

The aim of this study was to measure EWLH by the single-wire capacitance probe under all the flow patterns in horizontal gas–liquid flows, and to analyze the measuring factors theoretically and experimentally. Based on the measurements, the information on flow structure and the concerned parameters were estimated such as interfacial velocities, phase distribution, void fraction, and flow patterns.

* Corresponding author.
E-mail address: shanfang_huang@mail.xjtu.edu.cn (S. Huang).

0301-9322/$ - see front matter © 2008 Elsevier Ltd. All rights reserved.
doi:10.1016/j.ijmultiphaseflow.2008.03.004

2. Measurement principle

2.1. Theoretical analysis and static validation

Fig. 1 expresses the structure and the static performance of the single-wire capacitance probe. In Fig. 1a, the dielectric of the capacitor is the insulating film, and the two electrodes are the metal core of the wire and the water over the surface, respectively. The capacitance C is calculated by

$$C = \frac{2\pi\varepsilon l_1}{\ln\frac{d_2}{d_1}} + \frac{2\pi\varepsilon l_2}{\ln\frac{d_2}{d_1}} + \ldots + \frac{2\pi\varepsilon l_n}{\ln\frac{d_2}{d_1}} = \sum_{i=1}^{n} C_i = k\sum_{i=1}^{n} l_i, \quad (1)$$

where l_i (i = 1,2, ... ,n) are the sections of water covering the wire. ε is the dielectric constant, d_2 and d_1 are the diameters of the wire with and without the film, respectively. The capacitance C is the parallel connection of C_1, C_2, ..., C_n formed by the water sections. Suppose that ε, d_1, and d_2 are fixed; then the coefficient $k = \frac{2\pi\varepsilon}{\ln\frac{d_2}{d_1}}$ is a constant. Therefore, the capacitance is proportional to the sum of the water layer heights contacting with the wire $l = \sum_{i=1}^{n} l_i$, namely EWLH. Additionally, the coefficient k is very high since $d_2 \approx d_1$ when the thickness of the insulation film is very small, which means that the probe has a high sensibility.

Water is used as an electrode of the capacitor in this method and the conductivity between the two electrodes is not measured directly, which is the substantial difference from the conductance probe. The single-wire capacitance probe is not limited to a straight line, but can be a curve with any shape. In addition, the probe can be placed perpendicular to or inclined to the pipe wall.

To a given capacitance C, the measured capacitance C_m by an instrument is always smaller than the actual value (Bao and Hu, 2001) due to

$$C_m = \frac{C}{1 + (wCR)^2}, \quad (2)$$

where ω is the measuring frequency, and R is the resistance in the measurement circuit. In this method, water is used as an electrode of the capacitor and water resistance is the determining part of R. Generally speaking, water salinity varies extremely great in industries with the range from 10 to $10^5\Omega$. Suppose that the order of magnitude of the capacitance is 10 pF and the working frequency ω is 1000 Hz. Then we obtain

$$10^{-7} < \omega CR < 10^{-3}. \quad (3)$$

Therefore, the difference between C and C_m is very small due to the variation of water conductance, with the relative error below 0.01%. From the deduction mentioned above, we can find theoretically that the measured capacitance is not influenced by the salinity at all. As to the conductance probes, they will be disabled completely under the same conditions.

To validate the linear relationship between the capacitance and EWLH in Eq. (1), static experiments were carried out at 20 °C with different salinities of 0%, 2%, and 5% in water, respectively. A straight wire was made of a copper cylinder with an even layer

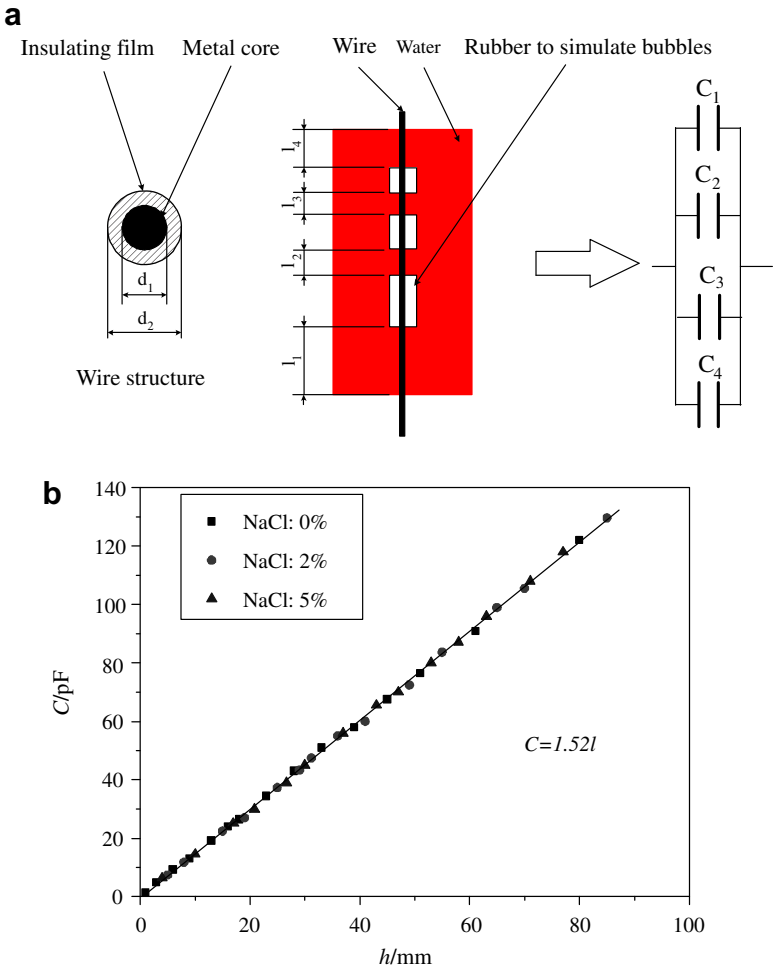

Fig. 1. A single-wire probe (d_2 = 0.17 mm): (a) structure; (b) static performance (20 °C).

of Teflon film. The layer of Teflon was plated over the wire to form a thin film with the same thickness all over the wire surface. The ready-made insulated wires with different sizes were prepared. After static testing, we selected the insulated wire for dynamic experiments, with the diameter of 0.17 mm and the coefficient of 1.52 pF/mm. The insulated wires used in static and dynamic experiments were the same. The linear relationship is always certain and the sensor will work well as long as the thickness of the insulating film is even over the whole wire. What is necessary to know is no more than the experimental coefficient of the probe.

Ten pieces of cuboid rubber to simulate bubbles, with each height over 10 mm, were randomly arranged over the wire surface. The experimental results are illustrated in Fig. 1b. It is seen that all the data at different salt concentrations fall in the same line, which indicates that capacitance is proportional to EWLH contacting with the wire and is independent of water salinity or the phase distribution away from the wire. The fitted line between capacitance and EWLH is as follows:

$$C = 1.52l. \tag{4}$$

The sensitivity of the probe, $k = 1.52$ pF/mm, is much higher than that of the non-intrusive capacitance probe. Then the experiments were repeated when the wire was curved with any shape, and the results were identical.

The flow structure and the concerned parameters such as phase distribution, void fraction, interfacial velocity, flow pattern, and even tomographic imaging, can be obtained when the probes are arranged with the similar patterns to the literatures (Shi and Kocamustafaogullari, 1994; Reinecke et al., 1998; Oddie et al., 2003).

2.2. Dynamic process

The single-wire capacitance probe used in this study is made of a thin wire stretched through the diameter of the pipe in the vertical direction, and a lead from water mounted flush with the bottom of the pipe. The dynamic process for the two-phase mixture to flow over the wire, which is in nature the process for one phase to replace the other, determines the response of the probe and the measuring accuracy.

The dynamic process can be decomposed into two parts in horizontal and vertical directions as shown in Fig. 2. In horizontal direction, the process is simplified as a bubble to flow over a circular cylinder, which is similar to the process for a bubble to flow over a needle-contact probe (Gherson and Lykoudis, 1984; Billingham and King, 1995; Cartellier and Barrau, 1998). It is composed of six steps in turn with the flow direction from the right to the left. For gas–liquid transition, the liquid inertia induces a surge of the interface before the liquid film breaks. On the other hand, gas is directly replaced by water without time delay for liquid–gas transition.

In vertical direction, water layer moves up and down over the wire surface. In the rising stage, the dynamic contact angle, called advancing angle γ_a, is larger than static contact angle γ_0. However, the dynamic contact angle, namely receding angle γ_r, is less than γ_0 when water is falling. When water layer rises, gas occupying the wire surface is easily replaced by water. The advancing angle γ_a varies as a function of contact-line velocity (Billingham and King, 1995), but the error due to surface tension is estimated small, with the order of the wire diameter. On the other hand, when water layer falls, the replacement process is much more difficult. A thin layer of water film will adhere to the wire surface when the area of water film is dramatically increased. Obviously, it is under an unstable state with high surface free energy. The water film covering the wire is stretched and would break if the surface free energy is higher than a critical value. After that process, it reaches a stable state when the water film breaks into discrete droplets. The droplets do not fall down the wire since the gravity is negligible. Because the droplets are discrete to the water layer at the pipe bottom, they would not contribute to the measurement of water layer height.

Many factors relevant to the fluids and the wire have effect on the process such as fluids' properties, wire size, inertia, wettability, and etc. Some of the parameters are qualitatively described as follows:

Wire diameter. Wire diameter is the most important factor to determine the process. A wire with small diameter will traverse small bubbles easily, which increases the detection capacity. To improve the measuring accuracy, it is always desirable to decrease the wire diameter as much as possible.

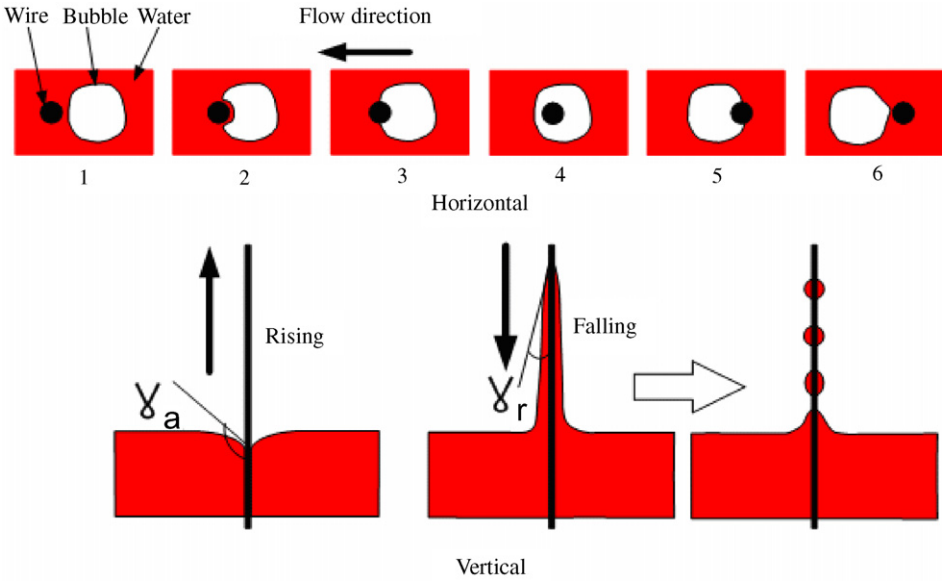

Fig. 2. Flow process of air–water two-phase flow over the wire.

Inertia. Water density is much larger than that of air, so the gas over the wire surface is easily replaced by water due to inertial effect, but the reverse process is difficult.

Wettability. The wetting effect determines the contacting form of water over the wire surface. Generally speaking, water, with the form of droplets, is more adsorptive to the wire surface.

From the above discussion, the water layer height measured by the single-wire probe will be overestimated due to the factors relevant to the fluids and the wire. However the error can be regarded as a constant. In dynamic experiments, two factors relevant to flow patterns, namely bubble size and interfacial propagation velocity, determine mainly the flow process and therefore the measuring error.

Bubble size. The process in horizontal direction is a common one, and the detailed processes are different with various bubble sizes. When the bubble size relative to the wire diameter is qualitatively large, the deformation of the bubble is small and the relative error of the measured EWLH may be negligible. On the other hand, when the bubble size is very small, it keeps the spherical shape and slips away from the wire without being pierced at all. Therefore, the bubble cannot be detected effectively with large error. Generally speaking, the ability for the wire capacitor to detect the bubbles becomes weaker when the bubble size decreases.

Interfacial propagation velocity. When the two-phase flow passes the wire, water will adhere to the wire surface and escape with a time delay due to wetting effect. For the given wire and fluids, the delay time may be treated as a constant. When the propagation velocity is big enough, it's too late for the front interface to be away when the rear one comes. Additionally, high propagation velocity will result in wake effect, where the gas will be trapped in the wake region behind the wire. This phenomenon vibrates the wire and increases the noise of the output signals. However, it will not bring obvious error since there is a thin film between the wake zone and the wire due to adhesion effect.

In dynamic experiments, we would pay main attention to bubble size and interfacial wave velocity when analyzing the measuring error.

3. Experimental setup and procedure

3.1. Experimental setup

The experimental setup in this study is reconstructed from that in Huang et al. (2007). The oil loop was replaced by an air loop and the quick-closing-valve system was taken away. Air was pumped by a compressor with a capacity of 0–6 Nm^3/min and stored in a gas tank with a constant volume, and the flow rate was metered by two glass-tube rotameters. Water was pumped by a stainless centrifugal pump with a capacity of 0–15 t/h, and its flow rate was metered by an electromagnetic flow meter and an orifice meter at different flow rates. The flow rates of air and water were controlled by respective bypasses. To minimize the disturbance to air–water mixture, gas and water were introduced into a stainless-steel mixing tank as stratified flow according to their densities, and then the mixture flowed into the horizontal pipe with the inner diameter of 29 mm. After the mixture flowed into the cyclone separator located at the end of the pipe, air was vented to the atmosphere and water entered the water tank for recirculation. To calculate the air superficial velocity accurately, it is necessary to know the in situ absolute pressures. Pressure transducers of the diaphragm type were utilized at three locations, i.e. in the two single-phase loops and in the main loop. In the experimental ranges, the maximum pressure was about 3 bars in the air loop and it was always near atmospheric pressure in the main loop. In order to observe the development of the flow process, the whole horizontal pipe, including the test section, was made of transparent acrylic resin.

The data acquisition system (DAS) and high-speed camera were the same as in Huang et al. (2007). The sampling frequency of DAS is 1000 Hz with the duration of 10 s for each flow condition. High-speed camera recorded the flow structures from the side view with the image refresh rate of 1000 or 2000 pictures per second according to different flow velocities in order to capture the details of the flow process.

The test section 1 m in length, was seamlessly connected with the main pipe and was located at about $L/D = 200$ from the mixing chamber. Fig. 3 describes the structure of the test section. Two identical single-wire probes spaced 120 mm apart were used to measure EWLHs, from which the propagation velocity was calculated by cross-correlation technique. Considering the small deformations and the disturbances generated by the probe, only the signals of the upstream probe were adopted as EWLH. The wire used in dynamic experiments was the same as that in the static experiments described in Section 2.2. The distance is 5 mm between the wire and the lead.

3.2. Experimental procedure and conditions

The flow conditions were specified by varying the flow rates of water and air. Gas flow rate was increased gradually while water flow rate was fixed at a constant value, and a series of the flow conditions were obtained. After that, the water flow rate was adjusted

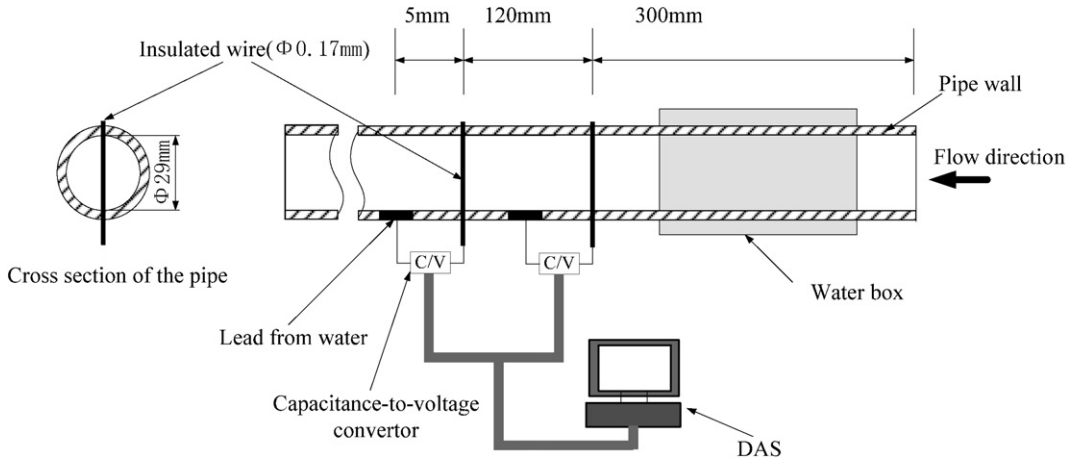

Fig. 3. Structure of the test section.

to another constant value and the former procedure was repeated; then another series of flow conditions were obtained. When the steady state was reached under each flow condition, the voltage outputs of the two probes were recorded simultaneously by the DAS and stored into the computer. Meanwhile, the high-speed camera recorded synchronously the continuous flow process from the side view.

The ranges of the superficial velocities were 0–5 m/s and 0–26 m/s for water and air, respectively. The experiments were carried out at about 20 °C under atmospheric pressure. The gas superficial velocities were computed at the in situ pressures of the measuring stations.

4. Results and discussion

4.1. Time traces in different flow patterns

The experimental results were discussed by the classification of flow patterns. The flows were divided into four patterns similar to Barnea et al. (1980), i.e. stratified, intermittent, bubbly, and annular flows. In order to compare the experimental results in different flow patterns, all the time traces of EWLH were shown within 1 s under the typical flow conditions.

4.1.1. Stratified flows

Andritsos and Hanratty (1987) measured water layer height in stratified gas–liquid flows in horizontal pipes and subdivided stratified flow into stratified smooth (SS), two-dimensional (2D), large amplitude (LA), and atomization (AT) flows according to the shape of interfacial waves. Shi and Kocamustafaogullari (1994) measured interfacial wave structures and obtained the similar results. In this study SS flows with an interface of flat horizontal plane were not observed. For a fixed liquid flow rate, three flow patterns, 2D, LA and AT flows, were visually observed in turn with gas flow rate increasing gradually. Fig. 4 shows the typical flow structures and the corresponding time traces under stratified flows. The superficial velocities of air and water are also marked.

In Fig. 4a, we can see that the curve and the flow structure are consistent very well in 2D flows, which is similar to be under the static condition. The measuring error can be negligible.

In Fig. 4b, the interfacial structure becomes irregular with large amplitude in LA wave. The wave is comprised of a fairly steep front and a long tail. The interface in front of the LA wave was rather smooth. The observed results were consistent well with the literatures (Andritsos and Hanratty, 1987; Sawai et al., 1989; Shi and Kocamustafaogullari, 1994). The time trace of EWLH can show the characteristics of the flow process. The error is estimated to be small since the wave propagation velocity, to be discussed below, is very small.

Fig. 4c illustrates the result of a typical AT wave. Above a certain gas velocity, the liquid began to climb up the upper wall of the pipe when the liquid droplets and the liquid filaments were torn from the liquid phase and deposited on the pipe wall. The interfaces before and behind the wave peak were wavier than in 2D flows. The water layer height behind the peak decreased gradually to the level before the peak. From Fig. 4c, it is seen that the EWLH at the wave peak measured by the probe are overestimated due to the filaments. When the AT wave passed the wire, the water filaments would cover the wire and depart from the surface with a time delay due to the adhesion effect discussed in Section 2.2.

4.1.2. Intermittent flows

Intermittent flow pattern is subdivided into plug and slug flows. The criterion to distinguish plug and slug is whether the liquid slugs are aerated. An intermittent unit consists of a slug region and a trailing film region. Fig. 5 shows the typical time traces of EWLH and the flow structure in intermittent flows.

In a plug flow as shown in Fig. 5a, the two pictures are the bubble head and the bubble tail respectively. The interface of the film region was calm and the liquid slug is almost free of entrained gas bubbles. The curve agrees well with the flow structure. The

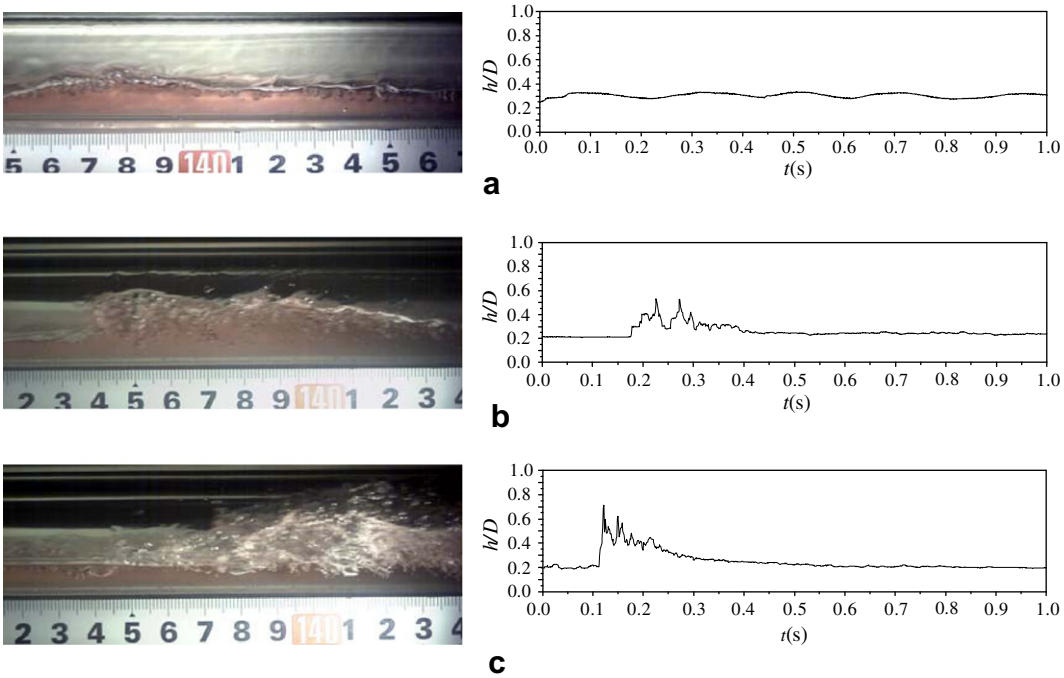

Fig. 4. Typical measurement results in stratified flows: (a) 2D wave (V_{SG} = 2.5 m/s, V_{SL} = 0.038 m/s); (b) LA wave (V_{SG} = 4.3 m/s, V_{SL} = 0.05 m/s); (c) AT wave (V_{SG} = 5.2 m/s, V_{SL} = 0.05 m/s).

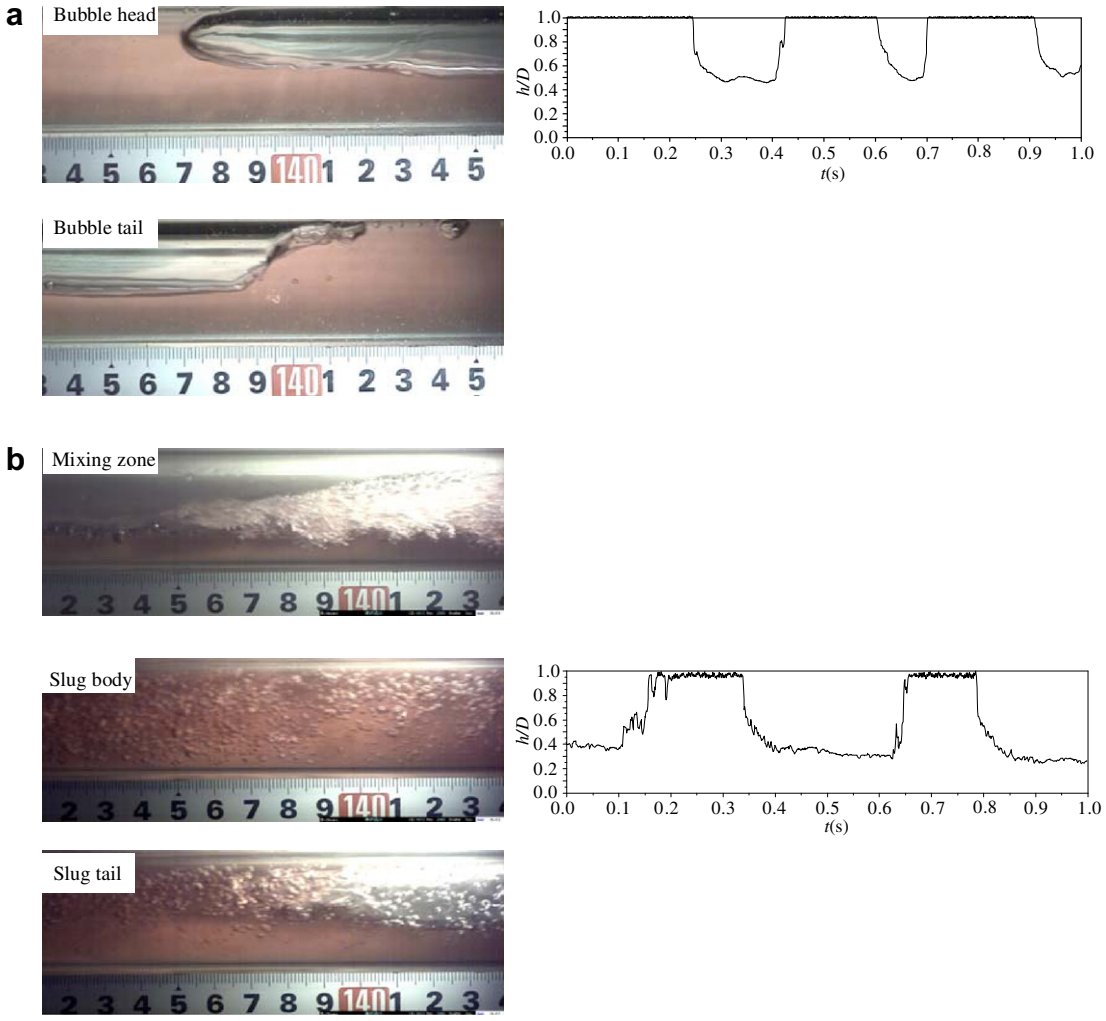

Fig. 5. Typical measurement results in intermittent flows: (a) Plug flow (V_{SG} = 0.14 m/s, V_{SL} = 0.56 m/s); (b) slug flow (V_{SG} = 1.71 m/s, V_{SL} = 0.92 m/s).

measuring error is estimated small because the liquid was free of discrete bubbles and the slug velocity was low.

Typical slug flow is shown in Fig. 5b. The slug region can be subdivided into three zones, which correspond to the three pictures. They are mixing zone, slug body and slug tail (Andreussi et al., 1993). In the mixing zone, there is a mixing vortex, where a large amount of gas is entrained. When the mixing zone passes the wire, the thin film entrained in the vortex will adhere to the wire surface and leave with a time delay due to adhesion effect, which overestimates the EWLH. In the slug body zone, the turbulence is dramatically reduced and the void fraction is much less than in the mixing zone. Thus the error was estimated to be much smaller. In the slug tail zone, the interfacial waves are similar to stratified structures, and the error is also small. In dynamic experiments, we observed the wake effect clearly when the liquid slug flowed over the wire at high velocities, but it will bring no measuring error. After the slug passed the wire, discrete water droplets were observed over the wire surface originating from the rupture of the water film.

4.1.3. Bubbly flows

Quite few studies have been conducted on the measurement of EWLH in bubbly flows. Fig. 6 presents a typical time trace of EWLH and the flow structure. The time trace fluctuates at high frequency and the EWLH is near unity. The measured EWLHs by the probe are obviously larger than the actual values because the bubbles hit the probes with high velocity and small ones slipped away from the wire. In most flow conditions, wake effects can be observed in bubbly flows due to high liquid velocity, but that would not bring obvious error.

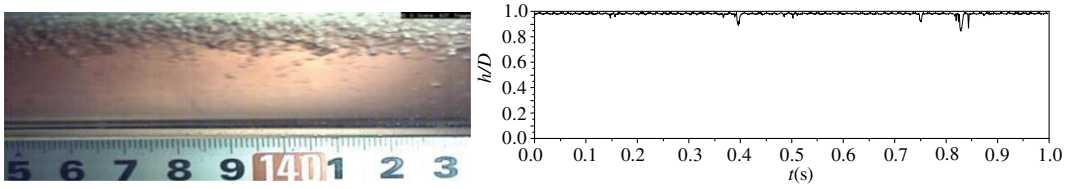

Fig. 6. Typical measurement result in bubbly flow (V_{SG} = 0.17 m/s, V_{SL} = 3.2 m/s).

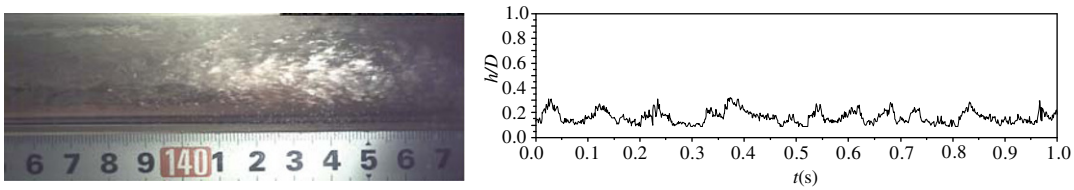

Fig. 7. Typical measurement result in annular flow (V_{SG} = 17.7 m/s, V_{SL} = 0.078 m/s).

4.1.4. Annular flows

In annular flows, most of the liquid is located at the bottom of the pipe and only a small amount is swept around to wet the pipe as a thin film. The typical time trace of EWLH, shown in Fig. 7, can roughly reflect the features of annular flows. Since the whole periphery of the pipe is covered with water film, it is impossible to observe clearly the process for the two-phase mixture to flow over the wire through high-speed camera. However, we can deduce the flow process on the basis of the analysis in Section 2.2. For example, occasional jumps in the time trace are the unique features of annular flows, which is due to the water droplets entrained by gas core. When the droplets hit the wire and stick to its surface continually, they would coalesce into a big one and then fall down the wire to the water layer at the bottom. At the moment that the big drop contacted with the water layer, there would be a jump in the time trace.

4.2. Comparison of the time traces in different flow patterns

From the experimental results in Section 4.1, the characteristics of the time traces of EWLH are different from each other in different flow patterns. The statistical parameters of the curves such as maximum, minimum and average can be used to characterize the flow processes, by which flow patterns can be identified. Table 1 summarizes the statistical parameters of the typical time traces in different flow patterns.

Average. As a whole, the time-averaged EWLH indicates the approximate liquid holdup over the cross section. From the experimental results, the dimensionless time-averaged height was obviously the largest in bubbly flows with the value of 0.985 and the smallest in annular flows with the value of 0.155. The averaged height in intermittent flow is generally larger than in stratified flow.

Maximum. The maximum of the curve reflects the peak position of the interfacial wave. In bubbly flow and in intermittent flows, the maximum is almost near unity because water bridges the top of the pipe; while in annular flow the maximum is the smallest. Among the three branches in stratified flows, 2D, LA and AT flows, the maximum height in AT flows was the largest.

Minimum. The minimum dimensionless EWLH in bubbly flows is the largest and is up to 0.8. The minimum in annular flow was the smallest, which may be smaller than 0.1. Generally speaking, the minimum is larger in intermittent flows than that in stratified flows.

Several other parameters of time traces such as amplitude, periodicity, and vibration frequency can also be used to describe the flow characteristics.

Table 1
Statistical parameters of the typical time traces

Flow pattern	V_{SG} (m/s)	V_{SL} (m/s)	Maximum	Minimum	Average
2D	2.5	0.038	0.344	0.256	0.298
LA	4.3	0.05	0.47	0.199	0.242
AT	5.2	0.05	0.722	0.188	0.251
Plug	0.14	0.56	1.02	0.41	0.824
Slug	1.71	0.92	0.998	0.263	0.546
Bubbly	0.17	3.2	1.00	0.819	0.985
Annular	17.7	0.078	0.34	0.089	0.155

4.3. Dimensionless time-averaged EWLH against superficial velocities

Fig. 8 illustrates the dimensionless time-averaged EWLH, $\bar{h}/D$, within the same sampling time of 10s under all the flow conditions. It is a function of superficial velocities. In stratified, bubbly and annular flows, experimental results of $\bar{h}/D$ are plotted as a function of V_{SG} where V_{SL} is treated as a parameter. However, when studying intermittent flows, only slug region is considered since the film region is relatively simple with the similar structures to those of stratified flows. As a whole, $\bar{h}/D$ decreases as V_{SG} increases or V_{SL} decreases in each flow pattern. However, the characteristics are different from each other in different flow patterns.

Fig. 8a shows $\bar{h}/D$ in stratified flows. The solid lines are the transitions from 2D to LA, and from LA to AT, respectively. The slope, indicating the decreasing rate of EWLH against gas superficial velocity, showed strikingly different behaviors in 2D and LA flows. A sharp decrease in $\bar{h}/D$ is observed in the transition region between 2D and LA regions, whereas the decrease is gradual in the LA region, which may be due to the liquid accumulation at the peak of the LA wave. Additionally, the large time interval between the sampled data will contribute to the sharp decrease. Compared with Shi and Kocamustafaogullari (1994), the time-averaged EWLHs are of the same trends, but the transition velocities are a little lower in this study. As a whole, the measured $\bar{h}/D$ is larger in this study especially in AT region. It may be due to the adhesion of the water filaments to the wire. Meanwhile, the fluctuation of the interface with high frequency increases the measuring error when the gas superficial velocity is high. Additionally, small water layer height cannot be measured by the intrusive probe when surface tension obviously comes into effect (Koskie et al., 1989).

Fig. 8b presents $\bar{h}/D$ as a function of mixture velocity in intermittent flows. In order to make comparison, the water holdups in the literatures are converted into EWLHs. Since the time trace of a slug has a finite slope at the front and the tail, the slug length depends on the discrimination level. From many investigations(Andreussi and Bendiksen, 1989; Andreussi et al., 1993; Fossa et al., 2003; Gopal and Jepson, 1997), it is seen that the converted EWLH is generally larger than 0.7. In this study, the dimensionless EWLH in time traces was set at 0.7 as the discrimination level to identify the beginning and the end of slug regions. The magnitude of the discrimination level would bring negligible error on slug length because the length of the sloping stages is much shorter than the whole liquid slug. The measured EWLH in the slug region was time-averaged by superposing all the slugs within 10 s. Comparing the results in this study with the literatures (Andreussi and Bendiksen, 1989; Fossa et al., 2003) in 40 mm i.d. pipes, they are consistent well at low mixture velocities. However, the measuring error of EWLH in this study becomes larger when the mixture

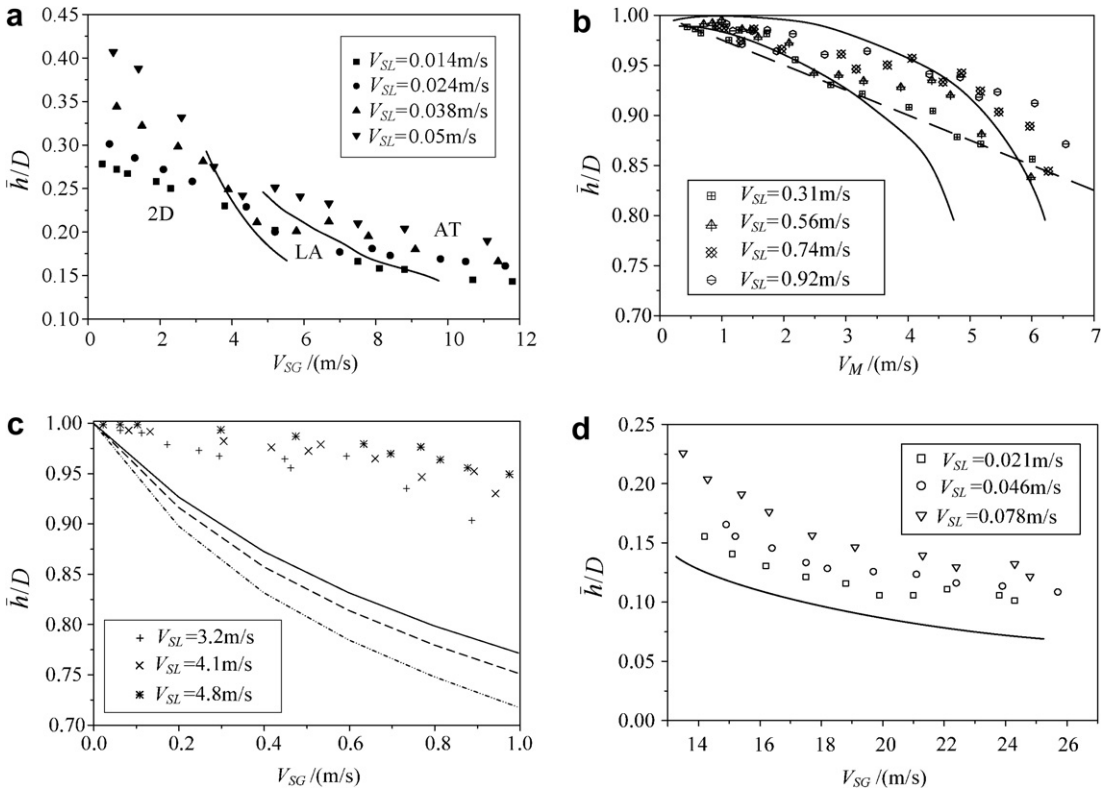

Fig. 8. Time-averaged EWLHs in all the flow patterns: (a) Stratified flows – Flow pattern transitions; (b) Intermittent flows — EWLH boundaries of Fossa et al. (2003) — EWLH of Andreussi and Bendiksen (1989); (c) bubbly flows — Theoretical EWLH at V_{SL} = 3.2 m/s – – – Theoretical EWLH at V_{SL} = 4.1 m/s –·–·– Theoretical EWLH at V_{SL} = 4.8 m/s; (d) annular flows — Experimental EWLHs at V_{SL} = 0.149 m/s (Lin et al., 1986).

velocity rises, because the detecting ability to the bubbles by the probe decreases as slug velocity increases.

Fig. 8c shows $\bar{h}/D$ trend in bubbly flows. The measuring errors of EWLH in this study were obviously large due to the disabled sensor in detecting small bubbles. In order to obtain the error in bubbly flows, theoretical EWLH is calculated based on the homogeneous model. The maximum error is about 28.6% in the experimental range.

In annular flows as shown in Fig. 8d, $\bar{h}/D$ tends to be constant with the limit of 0.1 as V_{SG} becomes high. While the limit in Lunisnki et al. (1983) is much lower than 0.1. The measured EWLHs are compared with the experimental results by pulsed photon activation (Lin et al., 1986), where the constant V_{SL} is 0.149 m/s with the pipe diameter of 26.9 mm. The measured EWLHs in this paper are obviously larger than those in Lin et al. (1986) with the maximum error of 50%. The interfacial wave fluctuates at high frequency due to high-speed gas core, so the vertical interfacial velocity is high, and the response velocity of the capacitance-to-voltage circuit is relatively low under annular flows. Additionally, water layer height around the circumference is small and the sensor is unreliable. The above three factors may overestimate EWLHs.

4.4. Interfacial velocities

The EWLHs were measured by the two probes upstream and downstream, by which the interfacial velocities can be measured

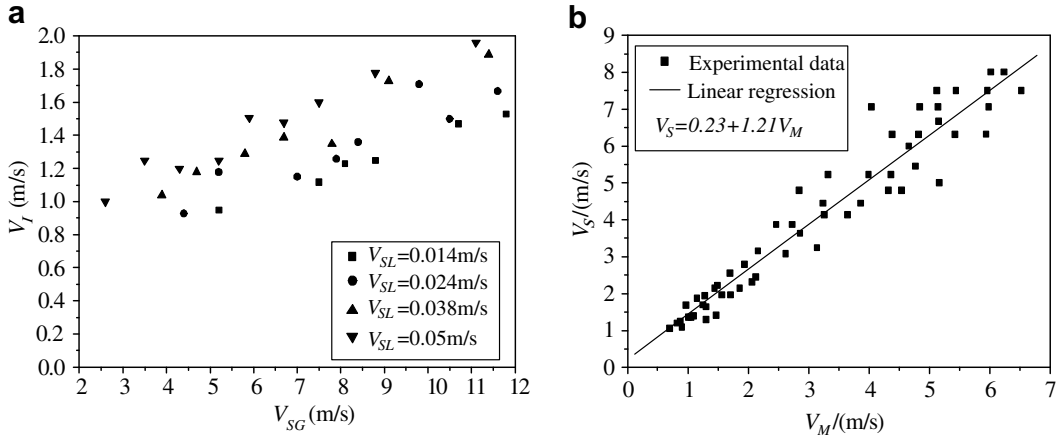

Fig. 9. Interfacial wave velocities: (a) Stratified flows; (b) intermittent flows.

based on cross-correlation technique in stratified and intermittent flows. However, the interfacial velocities cannot be measured in bubbly and annular flows because the flow structures are symmetrical with weak relativity along the pipeline. Fig. 9 illustrates the mean interfacial velocities in stratified and intermittent flows.

In stratified flows, the interfacial velocities V_I against V_{SG} are shown in Fig. 9a where V_{SL} is a parameter. Only the propagation velocities higher than 0.9 m/s can be measured in this study. For a given V_{SL}, the wave velocity linearly increased with V_{SG}. The maximum velocity was about 2.0 m/s in the experimental ranges, which is a little larger than in Shi and Kocamustafaogullari (1994).

Many investigations have been carried out to measure slug velocities (Nicholson et al., 1978; Bendiksen, 1984; Reinecke et al., 1998; Van Hout et al., 2002), and a linear correlation has been found. In this study, the mean slug velocities are plotted against the mixture velocity as shown in Fig. 9b. A linear correlation for the data may be obtained

$$V_S = C_0 V_M + V_0 = 1.21 V_M + 0.23 \quad (5)$$

The slope C_0 of the linear regression is comparable to those in the literatures within the range of 1.1–1.5. The range of the slug velocity considered in this study was about 1–8 m/s. Comparing Fig. 9a and b, we can see that, as a whole, the interfacial velocities in intermittent flows are obviously much higher than in stratified flows.

4.5. Comparison of the measurements in kerosene–water and air–water flows

Differences are found in measurement of EWLH by the single-wire capacitance probe in air–water and kerosene–water flows. Firstly, the flow processes are completely different in the two kinds of two-phase flows. There exist large differences in shape, size and superficial velocity between air bubbles and oil ones, which results in different flow pattern maps; Secondly, the processes are completely different for air bubbles and oil ones to pass the insulated wire from experimental observations and theoretical analyses. The differences mentioned above are mainly due to the different properties such as density and interfacial tension.

Density. Water density is much larger than that of air, so air is much more easily replaced by water over the wire surface than the reverse process due to inertial effect. This increases the measuring values of EWLH in dynamic experiments. While the difference between the densities of water and kerosene is much smaller, the process for kerosene to be replaced by water is comparable to the reverse one. Therefore, the measuring error resulting from density difference in kerosene–water flows can be estimated to be small.

Interfacial tension. The three-phase line, namely the contacting form of the fluids over the wire, is determined by interfacial tension. In kerosene–water flows, kerosene prefers to adhere to the wire surface, so water is more easily replaced by kerosene than the reverse process, which may result in negative error for kerosene–water flows. However, the interfacial tension, as one kind of the forces between molecules, is very weak compared with the inertial force. Therefore, the error caused by interfacial tension can be always estimated to be small. While in air–water two-phase flows, water prefers to adhere to the wire surface and the measuring error is always positive because of interfacial tension. Additionally, interfacial tension determines the sizes of air and oil bubbles, which has direct effect on the performances of bubbles.

5. Conclusions

The EWLHs were measured by a single-wire capacitance probe for all the flow patterns in horizontal gas–liquid flows. On the basis of the theoretical and experimental investigations presented in this study, the following conclusions may be drawn:

1. In static experiments, the measured capacitance is proportional to the EWLH contacting with the wire and independent of water salinity, phase distribution or wire shape. The probe used in this study has a high sensibility of 1.52 pF/mm. Several parameters, such as phase distribution, void fraction, interfacial velocity, and flow pattern can be obtained.
2. When the wire and the fluids are given, two factors relevant to flow pattern, namely bubble size and the interfacial velocity, influence mainly the measuring accuracy in dynamic experiments. The measured EWLHs are always larger than the actual values in gas–liquid flows and the error becomes larger when the bubble size decreases or the interfacial velocity increases. The measuring accuracy is high in stratified and intermittent flows and is low in bubbly and annular flows.
3. The statistical parameters of the time traces, namely average, maximum and minimum, vary with different flow patterns, which can reflect the flow characteristics.

Further work should be carried out to check the influence of wire size variation on the measurements. Other statistical techniques, such as probability distribution function, fast Fourier transform, and power spectrum, may be used to analyze the time traces of EWLH in order to obtain more information.

Acknowledgement

The authors gratefully acknowledge the financial support of a Foundation for the Author of National Excellent Doctoral Dissertation of PR China (FANEDD) (Grant No. 200337).

References

Andreussi, P., Bendiksen, K., 1989. An investigation of void fraction in liquid slugs for horizontal and inclined gas liquid pipe flow. Int. J. Multiphase Flow 15, 937–946.

Andreussi, P., Bendikson, K.H., Nydal, O.J., 1993. Void distribution in slug flow. Int. J. Multiphase Flow 19, 817–828.

Andritsos, N., Hanratty, T.J., 1987. Interfacial instabilities for horizontal gas–liquid flows in pipelines. Int. J. Multiphase Flow 13, 583–603.

Bao, X., Hu, M. (Eds.), 2001. Introduction to Electronic Apparatus. Beijing Technology University Press, Beijing. in Chinese.

Barnea, D., Shoham, O., Taitel, Y., 1980. Flow pattern characterization in two phase flow by electrical conductance probe. Int. J. Multiphase Flow 6, 387–397.

Bendiksen, K.H., 1984. An experimental investigation of the motion of the long bubbles in inclined tubes. Int. J. Multiphase Flow 10, 467–483.

Billingham, J., King, A.C., 1995. The interaction of a moving fluid/fluid interface with a flat plate. J. Fluid Mech. 296, 325–351.

Cartellier, A., Barrau, E., 1998. Monofiber optical probes for gas detection and gas velocity measurements: conical probes. Int. J. Multiphase Flow 24, 1265–1294.

Conte, G., Azzopardi, B.J., 2003. Film thickness variation about a T-junction. Int. J. Multiphase Flow 29, 305–328.

Fagundes Netto, J.R., Fabre, J., Peresson, L., 1999. Shape of long bubbles in horizontal slug flow. Int. J. Multiphase Flow 25, 1129–1160.

Fossa, M., Guglielmini, G., Marchitto, A., 2003. Intermittent flow parameters from void fraction. Flow Meas. Instrum. 14, 161–168.

Gherson, P., Lykoudis, P.S., 1984. Local measurements in two-phase liquid–metal magneto-fluid-mechanic flow. J. Fluid Mech. 147, 81–104.

Gopal, M., Jepson, W.P., 1997. Development of digital image analysis techniques for the study of velocity and void profiles in slug flow. Int. J. Multiphase Flow 23, 945–965.

Huang, S.F., Zhang, X.G., Wang, D., Lin, Z.H., 2007. Water holdup measurement in oil–water two-phase flows. Measur. Sci. Technol. 18, 3784–3794.

Kang, H.C., Kim, M.H., 1992a. The development of a flush-wire probe and calibration method for measuring liquid film thickness. Int. J. Multiphase Flow 18, 423–437.

Kang, H.C., Kim, M.H., 1992b. Measurement of three-dimensional wave form and interfacial area in an air–water stratified flow. Nucl. Eng. Des. 136, 347–360.

Koskie, J.E., Mudawar, I., Tiederman, W.G., 1989. Parallel-wire probes for measurement of thick liquid films. Int. J. Multiphase Flow 15, 521–530.

Lin, T.F., Block, R.C., Jones, O.C., Lahey, R.T., Murase, M., 1986. Horizontal annular flow measurements using pulsed photon activation and film thickness distribution modeling. Nucl. Eng. Des. 95, 353–363.

Luninski, Y., Barnea, D., Taitel, Y., 1983. Film thickness in horizontal annular flow. Can. J. Chem. Eng. 61, 621–626.

Nicholson, M., Aziz, K., Gregory, G.A., 1978. Intermittent two-phase flow in horizontal pipes: predictive model. Can. J. Chem. Eng. 56, 653–663.

Oddie, G., Shi, H., Durlofsky, L.J., Aziz, K., Pfeffer, B., Holmes, J.A., 2003. Experimental study of two and three phase flows in large diameter inclined pipes. Int. J. Multiphase Flow 29, 527–558.

Reinecke, N., Petritsch, G., Boddem, M., 1998. Tomographic imaging of the phase distribution in two-phase slug flow. Int. J. Multiphase Flow 24, 617–634.

Sawai, T., Yamauchi, S., Nakanishi, S., 1989. Behaviors of disturbance waves under hydrodynamic non-equilibrium conditions. Int. J. Multiphase Flow 15, 341–356.

Shi, J., Kocamustafaogullari, G., 1994. Interfacial measurements in horizontal stratified flow patterns. Nucl. Eng. Des. 149, 81–96.

Van Hout, R., Barnea, D., Shemer, L., 2002. Translational velocities of elongated bubbles in continuous slug flow. Int. J. Multiphase Flow 28, 1333–1350.